JMEPEG (1996) 5:260-268

A New Tensile Testing Procedure for Predicting Transverse Cracking Susceptibility of Continuous Casting Slabs

T. Revaux, J.P. Bricout, and J. Oudin

The testing facility used for simulation procedures of the thermomechanical history of continuously cast slabs before the straightening operation is described. The tests were made on in situ solidified specimens to reproduce the continuously cast microstructure and to follow the temperature history of the continuous casting process. The basic principle and procedure of the test are explained. The hot ductility curves and microstructures obtained are discussed for the approximate temperature range 700 to 1100 °C. Results are compared with one another and with other tensile test data.

Keywords

continuous casting, crack-temperature path, hot ductility, in situ melting, tensile test

1. Introduction

POTENTIAL advantages of the continuous casting of steel include the possibility of hot charging and direct rolling immediately after casting, which precludes conventional surface inspection at room temperature. A defect-free surface becomes a prime requirement for the economic production of slabs. Unfortunately, one problem that applies specifically to the continuous casting of steel remains transverse cracking, which occurs when the vertical cast strand is straightened. The transverse cracks are generally fine and can penetrate to an approximate depth of 5 to 8 mm below the surface.

The straightening operation is carried out in the temperature range from 1000 to 700 °C, which corresponds with the interval in which steels exhibit poor ductility in standard laboratory hot tensile tests. The relation between hot ductility behavior in tensile testing and the occurrence of transverse cracking in the straightening operation has led to intensive studies, which have alleviated this problem to some degree. Excellent reviews on cracking in relation to continuous casting were published, such as the early survey by Lankford (Ref 1) and the more recent publications by Thomas et al. (Ref 2), Maehara et al. (Ref 3), and Mintz et al. (Ref 4). However, on a more fundamental level, standard laboratory hot tensile tests do not accurately simulate the straightening operation in continuous casting. A major disparity is the degree of straining involved. In the straightening operation, it is at most only 1 to 2%, whereas in a hot ductility test, the fracture strains are often in the 10 to 100% range when tested at low strain rates. Thus, the mechanisms occurring during standard tensile tests do not necessarily coincide with those associated with transverse cracking. Moreover, the usual laboratory tests do not reproduce the actual temperature history of continuous casting of steels during current production processes because the deformation is often achieved on tensile specimens reheated from room temperature.

In spite of everything, because field research in production plants is possible only to a limited extent, the suitable approach remains the application of objective simulation procedures in the laboratory. Because metallurgical structure and hot ductility of continuous casting steels mainly depend on temperature history after solidification, developing a testing procedure more representative of temperature path and metallurgical structure before the straightening operation is important.

T. Revaux, J.P. Bricout, and **J. Oudin,** Industrial and Human Automatic Control and Mechanical Engineering Laboratory, C.N.R.S. Research Unity D1775, MECAMAT, Université de Valenciennes et du Hainaut Cambrésis, BP 311, 59304 Valenciennes, Cedex France.

2. Laboratory Hot Tensile Tests

Today, the most adequate and most used method for studying hot ductility is the hot tensile test, where reduction in area at the final rupture is taken as a measure of the hot ductility. For the study of transverse cracking, specimens are usually heated to a temperature above the solution temperature in the 1300 to 1350 °C range, both to dissolve all the microalloy precipitates and to produce a coarse grain size (Ref 5 to 10), and cooled to test temperature at a rate similar to that undergone by the continuously cast strand (60 to 100 K/s). Testing is then carried out at a strain rate comparable to that experienced during straightening; i.e., approximately 10^{-3} to 10^{-4}/s. However, the microstructure at the testing temperature obtained in this way may differ considerably from the microstructure obtained if the material is first allowed to solidify and then to cool to testing temperature directly. The differences in microstructure can entail that the material will display different ductility and strength values. Consequently, more sophisticated simulations of the continuous casting operation involve actually melting the samples. The expression "in situ solidified" is commonly used for the tensile test specimen cooled directly from the liquid phase to the testing temperature.

The Gleeble machine (Dynamic Systems Inc., Route 355, P.O. Box 1234, Poestenkill, NY 12140) is most often used because of its ability to melt a sample and its versatility in simulating the thermal cycle. In this case, heating is by electrical resistance, which has the advantage that there is no practical limit to the possible heating rate, and temperature gradients can be kept to a minimum. The molten material was kept in place using a quartz tube around the test rod (Ref 11). See Fig. 1. This

process was used for more than fifteen years by Suzuki et al. (Ref 12) for simulating the continuous casting of steel. Even though the method was perfected, this test still shows many problems (Ref 10): gravitation collapse of the liquid, incomplete fusion of the specimen, shrinkage cavity formation, and lack of repeatability.

Other testing equipment is available to obtain the high temperatures required. Singer and Cottrell (Ref 13) used a resistance heated furnace around a tensile testing machine. Trubisyn and Vasilevski (Ref 14) cast tensile test rods in a mold placed in a tensile testing machine. Kinoshita, Kasai, and Emi (Ref 15) applied an induction coil around a tensile test rod fitted in a tensile testing machine. B. Rogberg (Ref 9) designed a heat source consisting of three gold-plated ellipsoidally shaped reflectors fitted to 800 W halogen lamps. The tensile specimen, which is 40 mm in length and 8 mm in diameter, is placed inside a quartz tube, and the melted zone is kept in place by its surface tension. More recently, J. Hertel et al. (Ref 16) designed interesting testing equipment in which a 20 mm in diameter and 110 mm in length specimen is placed in a tightly fitting alumina tube to prevent an outflow of the melt (Fig. 2). However until now, despite wide experimentation, the tensile tests after remelt heat do not allow objective investigations, essentially because of the incidence of the shrinkage cavity (Ref 12, 15, 17). Therefore, prior investigations consisted of designing a laboratory hot tensile test on an in situ solidified sample with shrinkage cavity shifted out of the deformation zone. The main purpose here is to produce a tensile testing specimen with the columnar crystal structure of continuously cast slab surface by simulating the thermal history of the process.

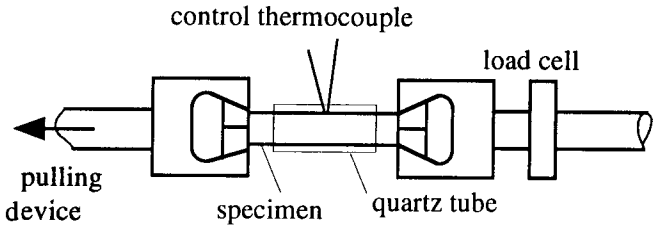

Fig. 1 Gleeble test

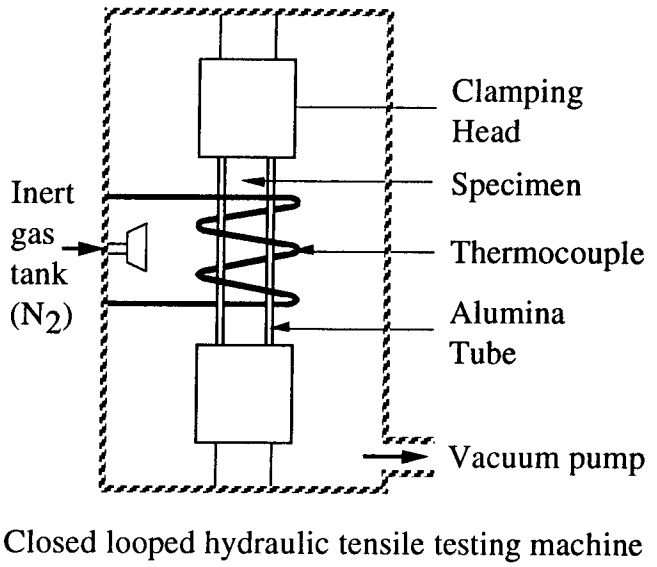

Fig. 2 Continuous casting simulator equipment

3. Tensile Testing Equipment

The basic principle of the test was fully explained in previous papers (Ref 18, 19). It involves melting a sample of the studied steel to obtain a notched tensile specimen. The test is then achieved at the required temperature, after a controlled cooling rate.

The starting specimen set consists of two round-bar blanks and a calibrated notched silica crucible; main dimensions are given in Fig. 3. By use of a cone-shaped silica crucible, the

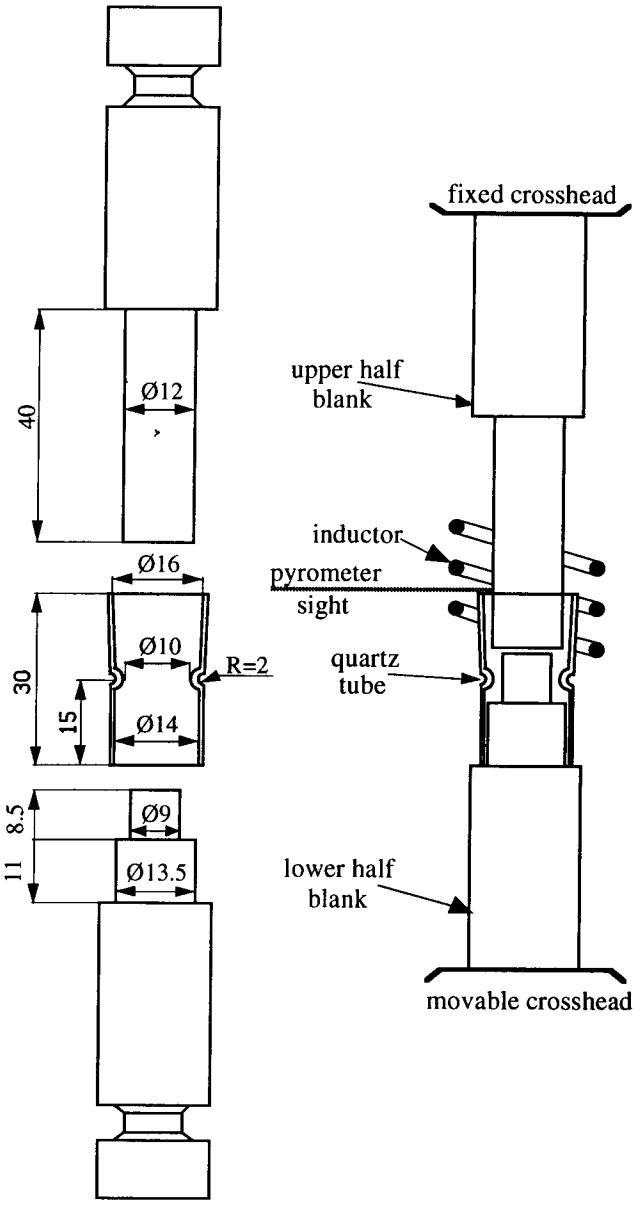

Fig. 3 Two blanks and silica crucible. The initial testing configuration

shrinkage cavity was shifted in the upper part of the crucible, about 10 mm above the notched zone. The troubles inherent in shrinkage cavity are avoided during stress measurements or during fracture surface analysis.

Figure 4 illustrates the three main sequences of the tensile test and shows the crucible and the parts of the two blanks, which are inside the inductor. The blanks are first heated at 20 °C/s up to 30 °C above liquidus in a flowing argon atmosphere to prevent occurrence of oxidation; the progressive raising of the testing machine lower ram allows the crucible to fill up (Fig. 4a). After 1 min holding in the liquid state, solidification occurs at a required cooling rate (15 °C/s) with a light compression of ~100 N to reduce the shrinkage cavity and cause the crucible destruction. Then, after the elimination of the crucible by using two sliding rods (Fig. 4b), the tensile test is carried out at a definite temperature, typically in the range of 700 to 1100 °C. Temperature is time controlled by a bicolored radiation pyrometer with optical fiber sighted between the turns of the induction coil (Fig. 4c). The used elongation rate is 0.25 mm/min, which corresponds to a mean strain rate defined as the elongation rate-initial notch width ratio of 10^{-3}/s. The thermal cycle of this testing procedure is schematized in Fig. 5(a) and referred to as "melting-procedure" or M procedure.

In comparison with the other remelting procedures, such as those using the Gleeble machine, the basic advantages of this test are (a) a complete remelting along the cross section of the sample, (b) a solidification without shrinkage cavity in the deformation zone of the sample, and (c) a reproducible geometry of the sample. Moreover,the notch favors microvoid growth and coalescence in producing depressive hydrostatic stresses.

For comparison, to assess the thermal history influence, some specimens were in situ solidified, cooled to room temperature, reheated to 1350 °C, held for 1 min, cooled at 15 °C/s to test temperature, held for 1 min, and tested to failure. The thermal cycle of this testing procedure is schematized in Fig. 5(b) and denoted as "reheating-procedure" or R procedure. The specimen geometry is identical for the R and M procedures. An accurate assessment of the temperature path influence is possible.

Table 1 gives the chemical compositions of the Nb (niobium) microalloyed steels used. Heats M1 and M2 are Nb containing steels, and heats M3 and M4 are Nb-V containing steels. Also note that heat M4 is high in V (vanadium) and contains a small amount of Ca (calcium).

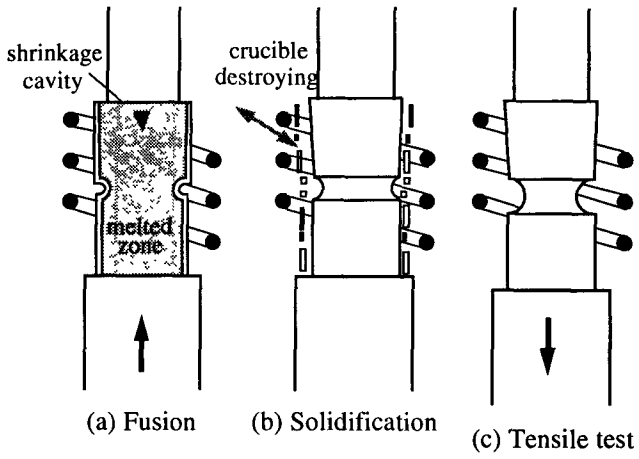

Fig. 4 Tensile test of in situ solidified notched specimens

4. Temperature Path and Metallurgical Structure

The influence of temperature path on metallurgical structure was studied on only heat M1. Metallographic examinations of the structures resulting from M and R procedures were realized both on longitudinal and cross sections in the notched zone after a continuous cooling to ambient temperature at a rate of 15 °C/s.

The cross-sectional micrograph in Fig. 6 clearly shows the strong influence of the temperature path on the size and morphology of the grains. Figure 6(a) shows the solidification structure of a specimen melted and then cooled at 15 °C/s to ambient temperature (M cycle). At the specimen surface, columnar grains are shown extended toward the specimen axis. In Fig. 6(b), the metallographic structure of a specimen treated in accordance with the R cycle shows a homogeneous structure with equiaxed grains. The grain size in the as-cast state is coarse and compares favorably with grain size measurements taken at the surface of continuously cast slabs. Reheating refines the grain size clearly.

The γ grain size measurements from the surface toward the axis of the specimen are given in Fig. 7. Prior γ grain size is measured easily because outlining by ferrite occurred during cooling. For the M specimens, the grain shape was charac-

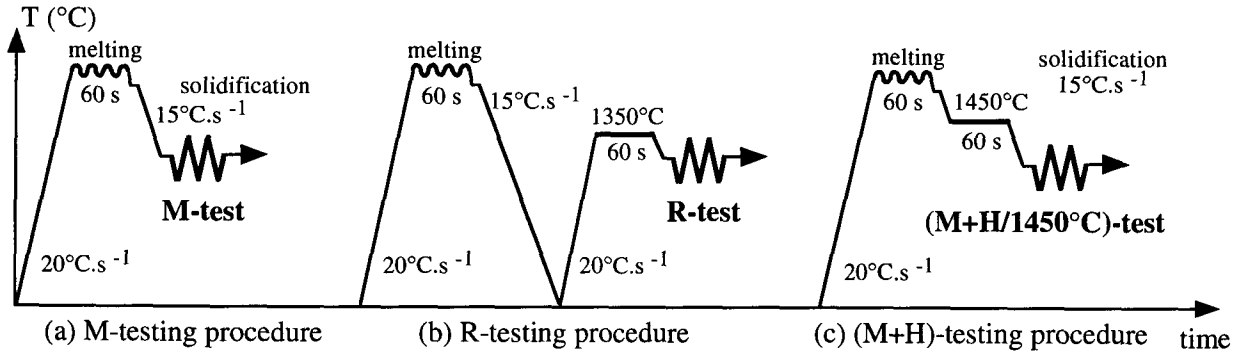

Fig. 5 Temperature histories: (a) tensile test of in situ solidified specimens (M test); (b) tensile test of in situ solidified, cooled, and reheated specimens (R test); and (c) tensile test of in situ solidified, held 1 min at 1450 °C specimens (M + H/1450 test)

terized by length (D), width (d), and the size factor (D/d). A 2 mm thick columnar region at the periphery and a finer, equiaxial grained zone at the center of the specimen are clearly identifiable (Fig. 7a). The columnar structure is caused by crystal growth that is perpendicular to the crucible surface during the solidification. As the austenitic grains are equiaxed for R specimens, the size factor, D/d, is 1 (Fig. 7b).

The interest of tests after remelting is shown here; the temperature path influence on the microstructure and, consequently, the size and location of the precipitates is indisputable. Moreover, since cracks are present at the slab surface and propagate inward, the presence of columnar grains at the sample surface is fundamental to reproducing the growth of transverse cracks.

Although the remelted tensile samples likely give results that are more closely related to the continuous casting process, this simulation does not perfectly fulfill all the characteristics of the straightening during continuous casting. In particular, the grain size near the surface of the continuously cast strand is likely to be 2 to 5 times larger than the one observed in remelted tensile samples. Therefore, the size and morphology of precipitates are also expected to differ from those observed at the strand surface. Thus, the M procedure must be modified to reproduce more precisely the grain size of continuously cast strand.

5. Temperature Path and Ductility

5.1 *C-Mn-Nb and C-Mn-Nb-V Microalloyed Steels*

In C-Mn (carbon-manganese) steels with no microalloying additions, the ductility trough is produced by strain concentration in thin films of the softer deformation induced ferrite, which surrounds the austenite grains. This strain concentration produces cavitation around the MnS inclusions; these cavitations link up to result in intergranular failure.

In microalloyed steels, the main mechanism of hot embrittlement is due to dynamic precipitation of nitride or carboni-

Table 1 Chemical composition of Nb-microalloyed steels

	Composition, wt %									
Heat	C	Mn	P	S	Si	Al	Nb	V	N	Ca
M1	0.113	1.468	0.014	0.005	0.492	0.05	0.033	0.001	0.016	...
M2	0.110	1.367	0.010	0.002	0.30	0.027	0.034	0.003	0.006	...
M3	0.106	1.334	0.010	0.002	0.29	0.027	0.033	0.024	0.004	...
M4	0.117	1.440	0.012	0.002	0.280	0.062	0.034	0.054	0.010	0.01

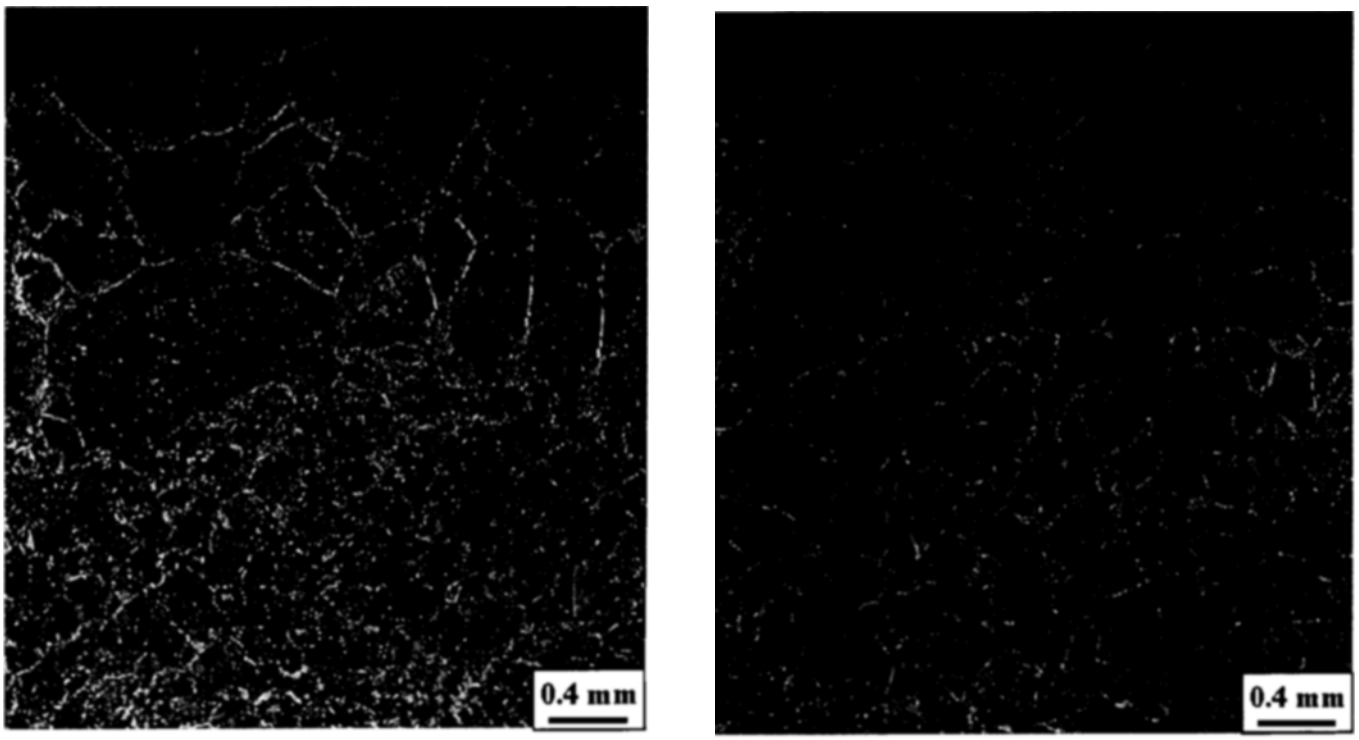

Fig. 6 Metallographic structures related to C-Mn-Nb steel (M1) after (a) M and (b) R tests. Radial sections level the notch of the sample.

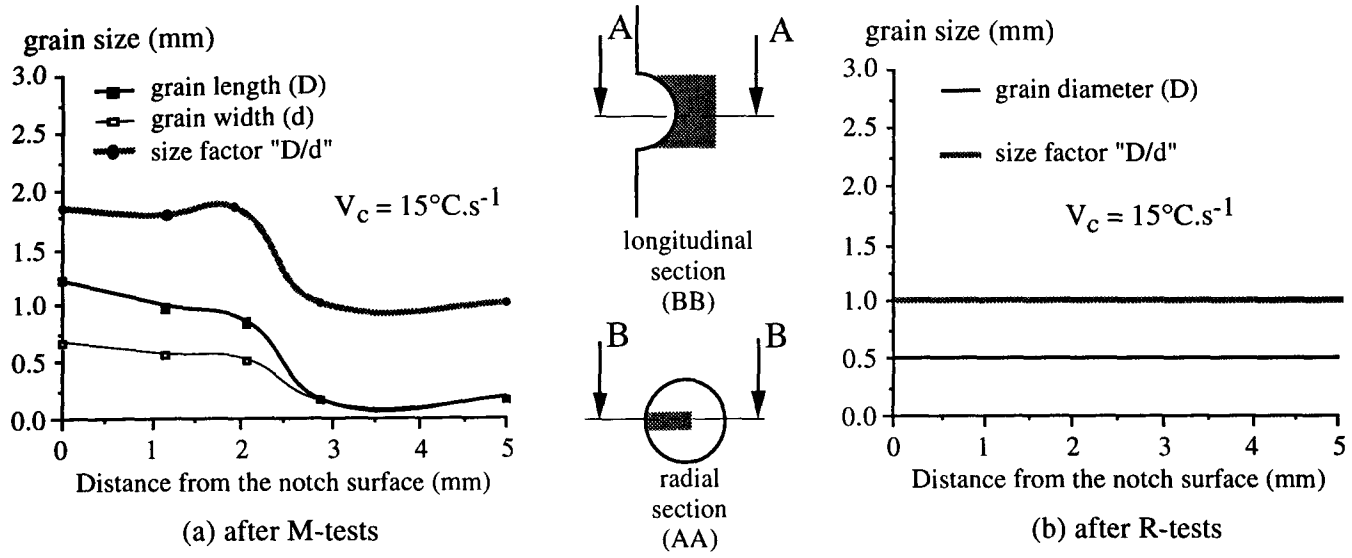

Fig. 7 γ grain size measurements from the surface to the axis (transversal section AA)

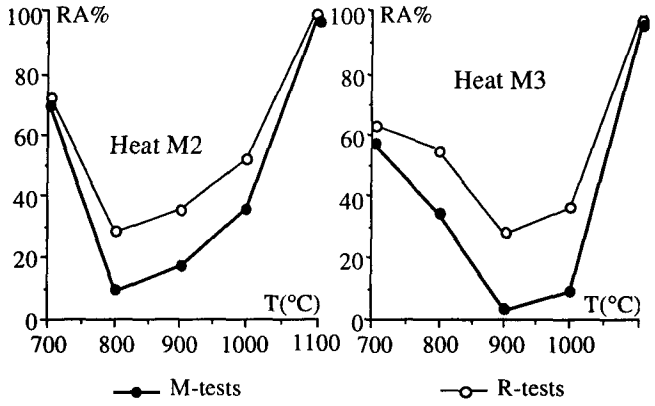

Fig. 8 Ultimate reduction in area versus temperature for C-Mn-Nb (M2) and C-Mn-Nb-V (M3) steels; 0.25 mm/min elongation rate

tride, such as AlN and Nb(C,N), which occurs at low strain rate in the temperature range of 700 to 1100 °C (Ref 20). The grain boundary precipitation that usually occurs is frequently accompanied by the formation of relatively weak, precipitate-free zones on both sides of the boundaries (Ref 21). Fine matrix precipitation also can take place and lead to significant matrix strengthening. The situation is then similar to the soft films of deformation-induced ferrite and leads to embrittlement in the single-phase austenite region by a combination of microvoid coalescence and grain-boundary sliding or shear. Thus, intergranular fractures are of mixed character and contain flat facets as well as coalesced microvoids (Ref 4). Furthermore, Y. Maehara and T. Nagamichi (Ref 20) showed that segregation of sulfur atoms to the grain boundary Nb(C,N) precipitate/matrix interfaces enhances decohesion and consequent nucleation of microvoids. Thus, ductility loss is reduced by decreasing sulfur content to less than 10 ppm.

Table 1 indicates the compositions of the two steels tested. Heat M2 is Nb containing steel, and heat M3 is Nb-V containing steel. Note that the S (sulfur) level is very low, and sufficient Mn is present to prevent classical hot shortness even under conditions far removed from equilibrium.

Figure 8 shows the ultimate reduction of area, RA = $(S - Sr)/S_0$. S_0 is the initial notch cross section, and Sr is the ultimate cross section, versus temperature for heats M2 and M3, and for M and R tests. Ductility clearly is strongly influenced by temperature history. The ductility trough is indeed deeper and wider for M tests. Note that RA values are nearly zero for M tests at 900 °C for heat M3. Moreover, for heat M3, note that the decay of ductility from higher temperatures is very sharp for both M and R tests. So, heat M3 will be more sensitive to transverse cracking if the straightening operation takes place in the temperature range of 900 to 1000 °C.

As for heat M1, the metallographic examinations of the unstrained zone of the tensile specimens showed that austenite grain size of in situ solidified specimens is always much coarser than for R specimens for both heats M2 and M3. (See Fig. 9.) Columnar grains perpendicular to the tensile direction are still present at the surface of the in situ solidified samples. The trough region is invariably associated with intergranular fracture. The fracture facets are covered with fine dimples or microvoids. (See Fig. 10.)

Precipitation is likely very affected by the solidification processes. Thus, the precipitate distributions in the as-cast specimen can differ from those occurring after solution treatment. Intense segregation of microalloying additions to the interdendritic boundaries probably occurs during solidification and will lead to interdendritic fracture and poor ductility. Such behavior would account for the importance of total sulfur level in controlling the hot ductility in the as-cast condition because the sulfur will segregate to the interdendritic boundaries during solidification and precipitate out at the γ-grain boundaries during cooling to the test temperature.

On the other hand, on reheating to 1350 °C, new γ-grain boundaries are produced away from the segregated areas. The sulfur redissolves at 1350 °C and subsequently reprecipitates out at these new boundaries that then control hot ductility. Since γ-grains are equiaxed and less coarse, the increase in spe-

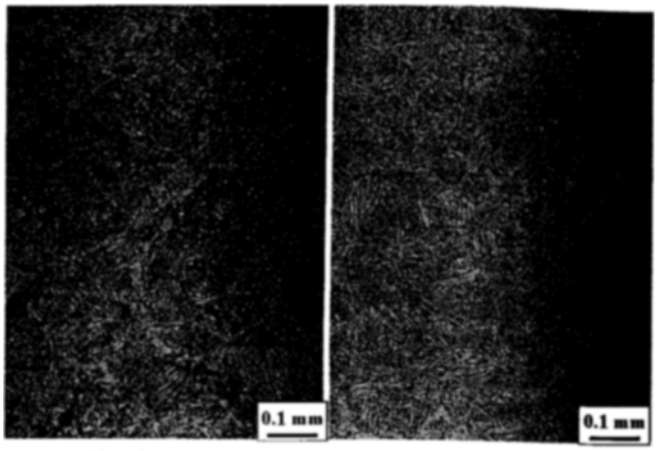

Fig. 9 Metallographic structures of the unstrained zone related to C-Mn-Nb steel (M2) strained at 1000 °C; 0.25 mm/min elongation rate

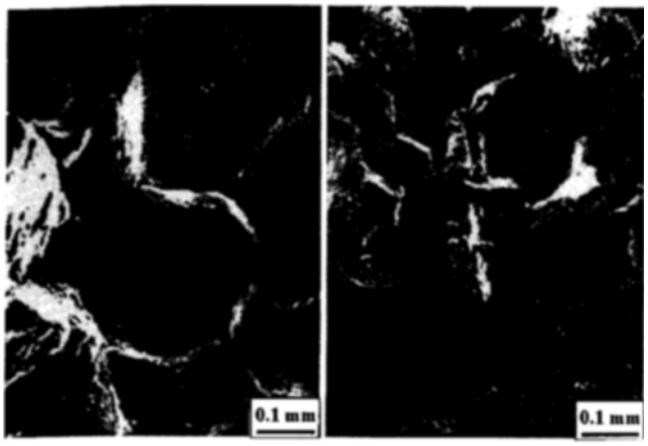

Fig. 10 Fracture surfaces related to C-Mn-Nb steel (M2) strained at 900 °C; 0.25 mm/min elongation rate

cific grain boundary area reduces also the precipitate density on the grain boundaries. Therefore, R procedure is less penalizing than M procedure for hot ductility of microalloyed steels.

In Nb-V containing steel (heat M3), the ductility loss due to Nb addition is also enhanced by the addition of V. So, the precipitation of VC(N) adds its detrimental effect to that due to NbC(N) precipitates (Ref 22).

5.2 *C-Mn-Nb-V/Ca Microalloyed Steels*

Previous works showed that the detrimental effect of sulfur on hot ductility depends on Mn and Ca contents (Ref 20, 23, 24). The mechanism usually considered is the embrittlement by precipitation of fine FeS particles, which segregate to the grain boundary during cooling or deformation. Mn additions replace them with MnS or (Fe,Mn)S particles formed at higher temperature, which are coarser, more spaced, less systematically intergranular, and less deleterious.

Ca has the same effect as Mn, but is more efficient. Ca additions are mainly beneficial because they reduce the volume fraction of sulfides formed on solidification as well as the amount of S precipitated in a finer form during cooling after solidification (Ref 24). Ca efficiency in relation to sulfur depends also on oxygen elimination by another addition (Ref 25). The favorable action of Ca on hot brittleness is different according to whether or not there are other additions. Ductility is not improved by an addition of Ca alone, but only when Ca is associated with Al (aluminum), which traps oxygen (Ref 26).

For heat M4 (C-Mn-Nb-V/Ca steel), hot ductility is not significantly influenced by the temperature path, and the ductility trough is more narrow than for Ca free steels, such as heat M3 (Fig. 11). For heat M3, the ductility trough is indeed clearly shifted toward the higher temperatures although the levels of Nb, V, N, and Al were lower than those of heat M4.

This behavior is explained by the fact that Ca reduces also solute S atoms in steel. Hot embrittlement due to sulfur was widely reported in the literature (Ref 3). If solute S atoms remain during low strain rate in the continuous casting of steel, they will segregate to the grain boundary precipitate/matrix in-

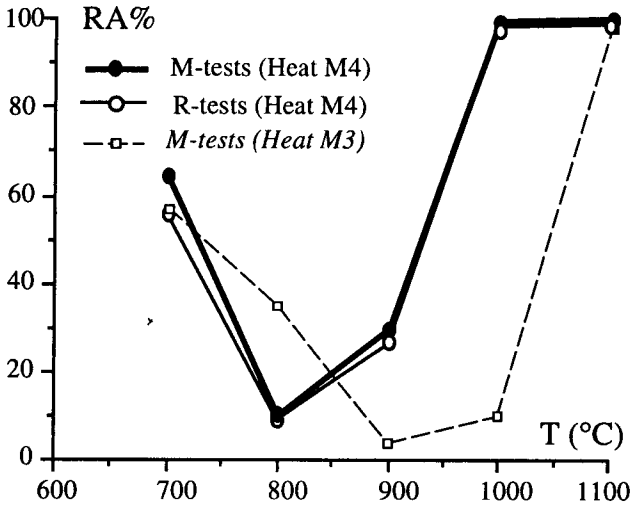

Fig. 11 Ultimate reduction in area versus temperature for C-Mn-Nb-V/Ca (M4) and C-Mn-Nb-V (M3) steels; 0.25 mm/min elongation rate

terfaces and to the austenitic grain boundaries, leading to easy decohesion of these interfaces and consequent nucleation of microvoids. With slow strain rates (10^{-3} to 10^{-4}/s, some investigators (Ref 27-29) believe that sulfur acts in the scope of a creep damaging process by segregating at the surface of the creep cavities located at the grain boundaries and strongly improves their growth velocity. The sulfur-intergranular precipitate synergy, which is often observed, results from the strong amplifier effect of these precipitates on cavity nucleation.

Thus, for steel solution treated at 1350 °C, the amount of S that goes back into the solution and then the part that remains in solution at the testing temperature could be effective in reducing the ductility. In as-cast steels, all the sulfur goes back into solution, and the solute S level at the testing temperature is higher than before. However, since the solute S level is very low in heat M4, there is no significant difference in hot ductility deduced from M and R testing procedures.

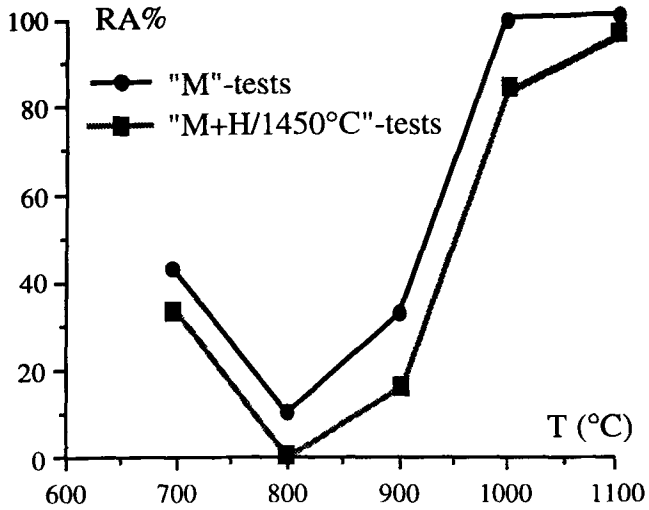

Fig. 12 Ultimate reduction in area versus temperature for C-Mn-Nb-V/Ca steel (M4); 0.25 mm/min elongation rate

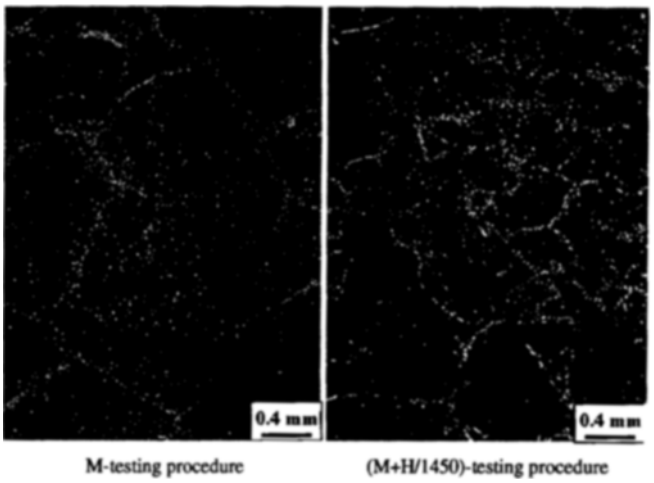

Fig. 14 Metallographic structures of the unstrained zone related to C-Mn-Nb-V/Ca steel (M4) strained at 800 °C and 0.125 mm/min elongation rate. After M test, V_c = 12 °C/s. After (M + H/1450 °C) test, V_c = 9.5 °C/s

In spite of everything, M tests might not precisely simulate the as-cast structure in continuous casting because the austenite grain size is more reduced in test. In continuous casting, the maximum surface strain on bending is about 2%, whereas the fracture strains are often higher than 5% with laboratory hot tensile test. Thus, the cracking conditions observed with current tensile tests are not necessarily those that occur during transverse cracking. To obtain a testing procedure capable of reproducing more precisely the as-cast structure in continuous casting, a melting procedure including a 1 min holding at 1450 °C was applied to heat M4 specimens (Fig. 5c).

Figure 12 shows the ductility curves for the melting and 1450 °C holding procedure, denoted as "M + H/1450," and for a simple melting procedure. The ductility curve relative to the M+H/1450 procedure is shifted toward the lower RA values. Note that RA is equal to zero at 800 °C.

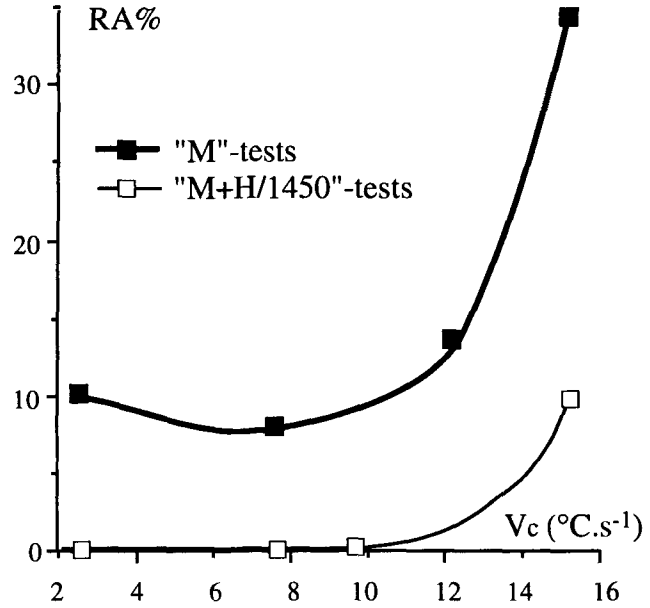

Fig. 13 Ultimate reduction in area versus cooling rate for C-Mn-Nb-V/Ca steel (M4) strained at 800 °C and 0.125 mm/min elongation rate. Influence of temperature path after in situ solidification

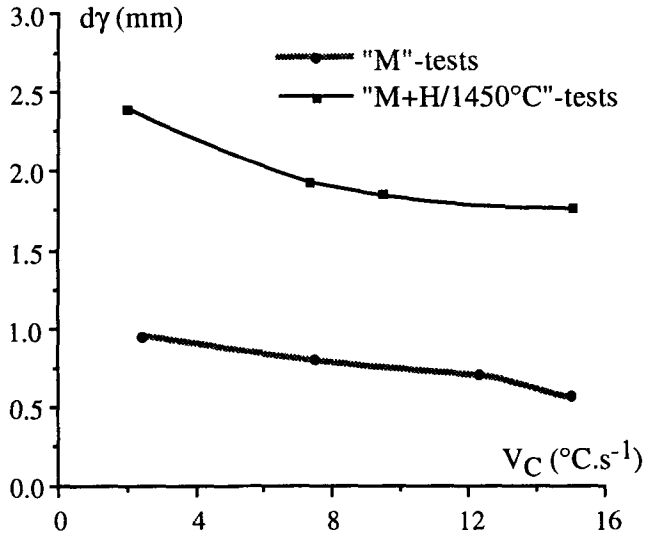

Fig. 15 Austenite grain size versus cooling rate for C-Mn-Nb-V/Ca steel (M4). Influence of cooling rate and temperature path on the austenite grain size at 800 °C

Figure 13 exhibits reduction in area versus cooling rate for heat M4 strained at 800 °C and 0.125 mm/min. Ductility is clearly influenced by temperature path and cooling rate. The ultimate reduction in area related to the M + H/1450 testing procedure is lower than the one related to the M testing procedure. For the M+H/1450 testing procedure, striction is nearly zero for cooling rates in the range 2 to 10 °C/s, which are typically the rates experienced by the strand surface during the continuous casting operation. Probably the mechanism giving intergranular cracks with test is now very close to the transverse surface cracking mechanism in continuous casting.

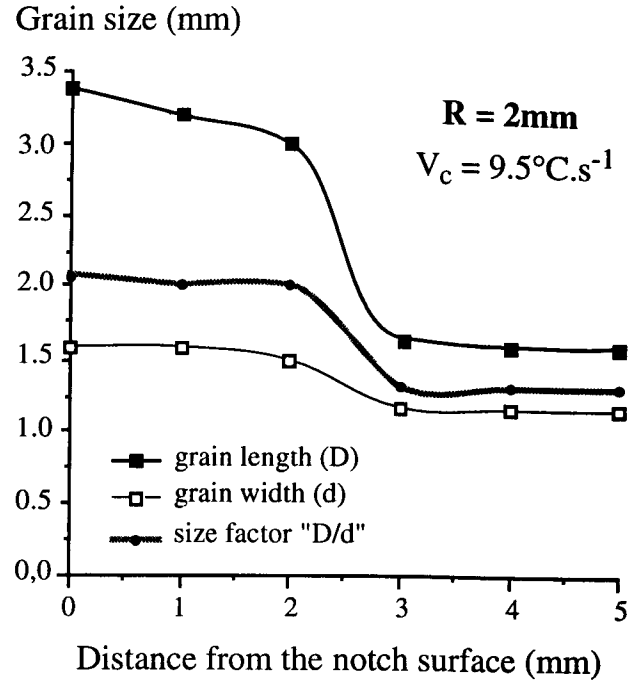

Fig. 16 γ grain size measurements from the surface to the axis after (M + H/1450 °C) test (transversal section AA)

The samples obtained from the M + H/1450 testing procedure, which have been subjected for a longer time at high temperature, are distinguished by a coarser structure as shown in Fig. 14 and 15. The after solidification 1450 °C holding allows the metallurgical structure of the continuously cast slab to be reproduced very precisely. Columnar grains are 3.2 mm in length and 1.6 mm in width as shown in Fig. 16.

The ductile character of the intergranular decohesion seems to be due to the necking of the no-segregated zones leading to the formation of ductile "ligaments" (Fig. 17, 18). The plainly intergranular fracture areas are due to an intense segregation of sulfur at the austenite grain boundaries and at the microvoid surfaces created around Nb(C,N) and V(C,N) particles located at the grain boundaries (Fig. 19). Moreover, raising the cooling rate induces a ductility increase because decreasing of the austenite grain size reduces the precipitate density on the grain boundaries.

6. Conclusions

As one aid in clarifying the mechanism of cracking in continuously cast slabs, a new tensile testing procedure was proposed. It includes melting and solidification in the form of notched specimens by simulating the slab thermal history. The choice of the specimen and crucible geometry was determined to shift the shrinkage cavity out of the notched zone and thus avoid any trouble during test measurements. It is a basic advantage in assessing stresses and strains for the analysis of surface fractures. Compared with other tests, the notched specimens offer a great interest in producing very depressive hydrostatic stress, producing significant triaxiality, and thus favoring microvoid growth and coalescence. The late step is quickly reached when the specimen notched zone has poor ductility.

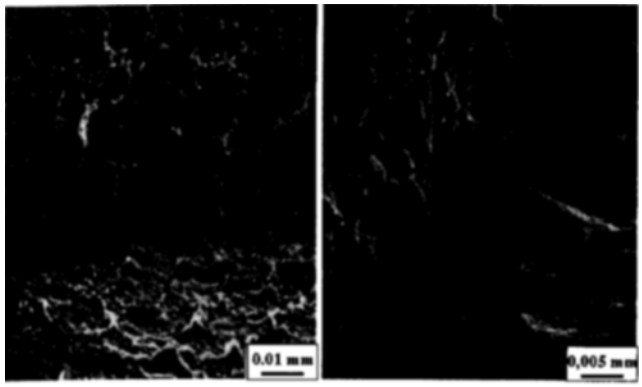

Fig. 17 Fracture surfaces related to C-Mn-Nb-V/Ca steel (M4) strained after (M + H/1450 °C) test at 800 °C and 0.25 mm/min elongation rate

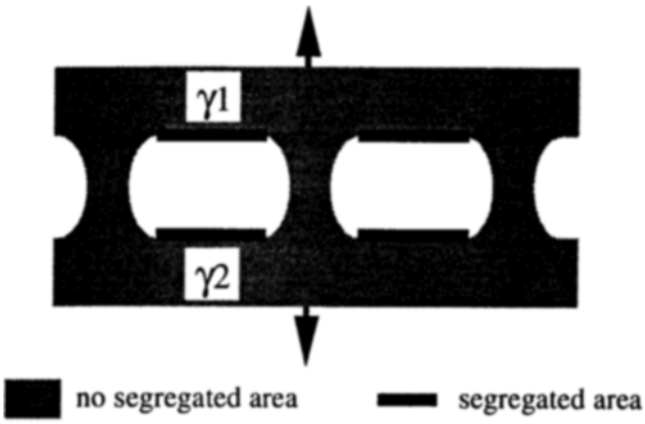

Fig. 18 Schematic representation of crack by plastic instability of the area between the voids leads to intergranular fracture facets with "craters"

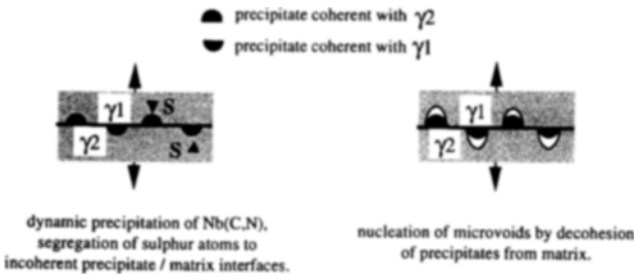

Fig. 19 Schematic representation of intergranular microvoid formation in Nb steel during low strain rate deformation in low temperature γ region

Hot ductility of Nb-microalloyed steels was analyzed in relation with temperature history after solidification. The gap between the in situ solidified procedure and the reheated procedure is very important and gives evidence of the temperature history effect on hot ductility. For Nb-V microalloyed steels, ductility loss due to Nb addition is enhanced by V addi-

tion. The ductility trough is deeper and shifted toward higher temperatures.

Ca treatment improves the hot ductility of in situ solidified samples probably because the total sulfur content is reduced.

The in situ solidified procedure, which includes a high-temperature holding step, produces a solidification structure with coarse columnar grains similar to the continuously cast microstructure. For C-Nb-V/Ca steel, this testing procedure gives reduced hot ductility because of grain coarsening and, more importantly, sulfur segregation on austenitic grain and carbonitride boundaries.

References

1. W.T. Lankford, Some Considerations of Strength and Ductility in the Continuous-Casting Process, *Metall. Trans.*, Vol 3, 1972, p 1331-1357
2. B.G. Thomas, J.K. Brimacombe, and I.V. Samarasekera, *Iron Steel Soc. Trans.*, Vol 7, 1986, p 7
3. Y. Maehara, K. Yasumoto, H. Tomono, T. Nagamichi, and Y. Ohmori, *Mater. Sci. Technol.*, Vol 6 (No. 9), 1990, p 793-806
4. B. Mintz, S. Yue, and J.J. Jonas, Hot Ductility of Steels and Its Relationship to the Problem of Transverse Cracking during Continuous Casting, *Int. Mater. Rev.*, Vol 36 (No. 5), 1991, p 187
5. M. Guttmann, The Hot Ductility Trough of Plain Carbon Steels and Its Impact on Various Types of Cracking in Continuous Casting. A Reevaluation of the Current Literature, *IRSID, MS RI 92-309*, Jan 1992
6. G.A. Wilber, R. Batra, W.F. Savage, and W.J. Childs, The Effects of Thermal History and Composition on the Hot Ductility of Low Carbon Steels, *Metall. Trans. A*, Vol 6, 1975, p 1727-1735
7. F. Weinberg, The Effect of Cast Structure on the Ductility of Steel Above 900 °C, *Metall. Trans. B*, Vol 14, 1983, p 285-289
8. H. Fuji, Steel Embrittlement Increase Just Above the Solidification Temperature, *Tetsu-to-Hagané*, Vol 64, 1978, p 2148-2157
9. B. Rogberg, An Investigation on the Hot Ductility of Steels by Performing Tensile Tests on in situ Solidified Samples, *Scand. J. Metall.*, Vol 12, 1983, p 51-66
10. X. Longaygue, Bibliographical Synthesis of Hot Tensile Tests after Refusion in-situ on Gleeble Machine, *IRSID, RI 92-325*, June 1992
11. W.F. Savage, *J. Appl. Polym. Sci.*, Vol 6, 1962, p 303-315
12. H.G. Suzuki, S. Nishimura, and S. Yamaguchi, *Tetsu-to-Hagane*, Vol 65, 1979, p 2038
13. A.R.E. Singer and S.A. Cottrell, *J. Inst. Met.*, Vol 73, 1947, p 33-54
14. N.A. Trubisyn and P.F. Vasilevski, *Russ. Casting Production*, Vol 6, 1969, p 286-289
15. K. Kinoshita, G. Kasai, and T. Emi, *Solidification and Casting of Metals*, The Metals Society, 1979, p 268-273
16. J. Hertel, H. Litterscheidt, U. Lotter, and H. Pircher, Laboratory Simulation of Strand Shell Stresses and Strains during Continuous Casting, *Rev. Métall., Cah. Inf. Tech.*, Jan 1992, p 73-81
17. G.A. Wilber, R. Batra, W.F. Savage, and W.J. Childs, *Metall. Trans. A*, Vol 6, 1975, p 1727-1735
18. P. Deprez, J.P. Bricout, and J. Oudin, Tensile Test on in-situ Solidified Notched Specimens: Effects of Temperature History and Strain Rate on the Hot Ductility of Nb and Nb-V Microalloyed Steels, *Mater. Sci. Technol.*, Vol A168, 1993, p 17-22
19. T. Revaux, P. Deprez, J.P. Bricout, and J. Oudin, In-situ Solidified Hot Tensile Test and Hot Ductility of Some Plain Carbon Steels and Microalloyed Steels, *ISIJ Int.*, Vol 34 (No. 6), 1994, p 528-535
20. Y. Maehara and T. Nagamichi, Effects of Sulphur on Hot Ductility of Niobium Containing Low Carbon Steels during Low Strain Rate Deformation, *Mater. Sci. Technol.*, Vol 7, 1991, p 915-921
21. B. Mintz, J.R. Wilcox, and D.N. Crowther, *Mater. Sci. Technol.*, Vol 2, 1986, p 589
22. H. Su, W. Zhang, and Z. Yan, Determination of the Kinetics of Carbonitride Precipitation in Austenite in C-Mn-V Steels Microalloyed with Ti, *Chin. J. Met. Sci. Technol.*, Vol 4, 1988, p 220-223
23. B. Mintz and Z. Mohamed, Influence of Manganese and Sulphur on Hot Ductility of Steels Heated Directly to Temperature, *Mater. Sci. Technol.*, Vol 5, 1989
24. B. Mintz and R. Abushosha, Effectiveness of Hot Tensile Test in Simulating Straightening in Continuous Casting, *Mater. Sci. Technol.*, Vol 8, 1992, p 171-177
25. S. Tsuge, *Proc. Int. Conf. on Stainless Steels* (Chiba), Iron and Steel Institute of Japan, 1991, p 799
26. C.J. MacMahon, Grain Boundaries Cohesion in Ferrous Alloys, *Communication Bolton Landing Conference*, 10-15 June 1974, CIT du CDS, No. 3, 1975
27. W.D. Nix, D.K. Matlok, and R.J. Dimelfi, *Acta Metall.*, Vol 25, 1977, p 195
28. M. Guttmann and P.H. Dumoulin, *Mater. Sci. Eng.*, Vol 43, 1980, p 249
29. L. Ben Mostefa Daho, G. Saindrenan, and M.P. Solignac, *Acta Metall. Mater.*, Vol 39, 1991, p 3111